Superconducting periodic nanostructures in a magnetic field

Paul Erdős*
School of Basic Sciences, Swiss Federal Institute of Technology, Lausanne, Switzerland
and School of Physics and Engineering, Sun Yat-sen University, Guangzhou, People's Republic of China

Wei Zheng
School of Physics and Engineering, Sun Yat-sen University, Guangzhou, People's Republic of China
(Received 25 October 2009; revised manuscript received 27 June 2010; published 27 October 2010)

Superconducting nanostructures in the form of square and hexagonal nets of conductors in an external magnetic field are theoretically investigated. The superconducting transition temperatures as functions of the field as well as the intricate patterns of the order parameter and current are determined using a minimization technique of the Ginzburg-Landau free-energy expression. Experimental results and the relationships with the tight-binding model of electrons on a lattice and with other problems are discussed.

DOI: 10.1103/PhysRevB.82.134532 PACS number(s): 74.78.Na, 74.81.Fa, 74.25.Ha, 74.62.−c

I. INTRODUCTION

In this paper we report theoretical results for superconducting nanostructures, (micronets), in an external magnetic field. Among the nanostructures graphene has been one of the most studied in the last decade and this also revived interest in hexagonal nanostructures, in general.

Parallel to the study of such real nanostructures a new field of research is concerned with the properties of Bose-Einstein condensates of cold atoms in optical lattices generated by laser beams. The condensates are subjected to an artificial magnetic field produced, e.g., by rotation of the optical lattice.[1,2]

The superconducting micronets, the bosonic system, as well as several other two-dimensional models such as Josephson junction arrays,[3] coupled spin arrays and electron hopping models show in many respects similar behavior. Therefore this work will also be relevant to the properties of these other systems.

The similarities in these systems ultimately are due their identical translational symmetry properties and to the breaking of this symmetry through the magnetic field which introduces phase factors into the relevant order parameters. A superconducting micronet consists of a planar lattice of wires made of superconducting material such that the wire diameter d is less than the penetration depth of an applied magnetic field. Therefore, in a micronet currents flow not only on the surface but also in the interior of the wires. Other than this condition, the dimensions of the wires may be arbitrary. We study square and hexagonal (honeycomb) nets with a constant and homogeneous magnetic field B applied perpendicular to the plane of the net. Our aim is to determine the superconducting transition temperature of the net and the pattern of supercurrents which may exist below the transition temperature, as a function of the magnetic field strength. Particular attention is given to finite or semi-infinite lattices. In contrast to the infinite lattices with periodic boundary conditions where solutions can only be obtained for fractional values of the magnetic flux per wire cell, in the latter case solutions can be obtained that are continuous functions of the flux and allow the study of transitions between different current patterns at eigenvalue crossings of the relevant equations.

An individual lattice unit bordered by a closed wire loop and not sectioned by any wire will be called a plaquette. All plaquettes are identical. The significance of the assumption that the wire diameter d be less than the penetration depth λ is that in the individual plaquettes of the net the magnetic flux ϕ need not be an integer multiple of the flux quantum $\phi_0 = ch/2e$. There is another characteristic quantity, the fluxoid ϕ, that is quantized in each plaquette.[4,5] defined as

$$\phi = \int_s \boldsymbol{B} \cdot d\boldsymbol{S} + \frac{m^* c}{4 n_s e^2} \oint \boldsymbol{j} \cdot d\boldsymbol{l} = q\phi_0, \quad q = \text{integer}. \quad (1)$$

The first term in Eq. (1) is the magnetic flux through the area S of the plaquette, the second term is, up to the prefactor, the line integral of the current density along a closed loop in the boundary wire of the plaquette, with n_s being the superconducting electron density. This contrasts to nets made of thick wires ($d > \lambda$), where $j=0$ deep inside the wire, so that the second integral in Eq. (1) vanishes. In that case the fluxoid reduces to the first term and the flux due to induced currents is always a multiple of ϕ_0.

This study will be restricted to a temperature range where the linearized Ginzburg-Landau (G-L) equations are approximately valid. However, the nonlinear term in the Ginzburg-Landau equations will be used when minimizing the free energy of the system. Further restrictions have also been found useful and will be introduced at the appropriate place in the text.

We wish to point out the interesting connection which exists between the superconducting micronet and the problem of electrons localized on the points of the same type of lattice as that of the micronet and hopping between the lattice points. Both problems lead to a mathematical model described by the Harper equations and therefore our results shed some light on these models, in general, as will be discussed in Sec. XI.

The problem of the square lattice was essentially solved by Wang,[6] in his doctoral dissertation (unpublished). His main results have been summarized in several papers[7–9] and are in good agreement with experimental findings. We extend his results to the cases of flux not treated by Wang and in-

troduce some different mathematical techniques. We also treat the case of a hexagonal lattice, for which the current pattern has not been investigated before.

II. FORMULATION OF THE BASIC EQUATIONS

In a superconductor in thermal equilibrium and in a stationary state the order parameter $\psi(x)$, whose squared modulus may be considered as the density of superconducting electrons, obeys the G-L equations[5]

$$\frac{\hbar^2}{2m^*}\left[\left(-i\nabla-\frac{2\pi}{\phi_0}\boldsymbol{A}\right)^2-\xi^{-2}\right]\psi+\beta|\psi|^2\psi=0 \tag{2}$$

with the boundary conditions

$$\left(-i\nabla-\frac{2\pi}{\phi_0}\boldsymbol{A}\right)\psi_b=0. \tag{3}$$

A is the electromagnetic vector potential, ϕ_0 the magnetic flux quantum, ξ the coherence length, and β is a phenomenological parameter (to be discussed in the section on energetics), m^* is an effective mass. The subscript b indicates the boundary. It was shown by Gorkov[10] that the G-L equations can be deduced from the microscopic BCS theory of superconductivity.

Linearization consists of the neglect of the third-order term in ψ in Eq. (2). This is legitimate at temperatures close to T_c because at the superconducting transition temperature T_c, ψ vanishes. The coherence length ξ depends on the temperature through

$$\xi(T)=\xi(T=0)[1-T/T_c(B=0)]^{-1/2}, \tag{4}$$

where $T_c(B)$ depends on the magnetic field B.

In thin wires ($d\ll\xi$), it is a good approximation to assume that the order parameter is constant within a cross section: at lattice points, where n wires (in our case $n=3$ or 4) meet, the following equation holds for all lattice points a

$$\sum_{b=1}^{n}\left(-i\frac{\partial}{\partial s}-\frac{2\pi}{\phi_0}A_s\right)\psi_{ab}(s)=0. \tag{5}$$

Here, s is the arc length along the wire and A_s is the component of A parallel to the wire at the point labeled by s. A detailed derivation of Eq. (5) is given in Ref. 11: it suffices to note here that condition (5) is the supercurrent analog of Kirchhoff's node equation.

As was shown by de Gennes,[12] the solution of the linearized G-L equation which gives the order parameter on a wire connecting the nodes a and b is given by

$$\psi_a(s)=\csc\left(\frac{l_{ab}}{\xi}\right)e^{i\gamma_{ab}(s)}\left[\psi_a\sin\left(\frac{l_{ab}-s}{\xi}\right)+\psi_b e^{i\gamma_{ab}(l_{ab})}\sin\left(\frac{s}{\xi}\right)\right], \tag{6}$$

where $s=0$ at a, and l_{ab} is the length of the wire $\overline{ab}$, ψ_a, and ψ_b are the order parameters in the two nodes and

$$\gamma_{ab}(s)=\frac{2\pi}{\phi_0}\int_{x_a}^{x(s)}\boldsymbol{A}(\boldsymbol{x})\cdot d\boldsymbol{s}, \tag{7}$$

where $\boldsymbol{x}$ is the position vector of a point on the wire. As will be seen later, $\gamma_{ab}(s)$ does depend on x_a and x_b as well as on s.

Equation (5) takes the form

$$\sum_b\left[-\psi_a\cos\left(\frac{l_{ab}}{\xi}\right)+\psi_b e^{-i\gamma_{ab}}\right]=0 \quad \text{for all } a. \tag{8}$$

If all wires have the same length l, and every lattice point has z neighbors connected to it, Eq. (8) reduces to

$$z\psi_a\cos\left(\frac{l}{\xi}\right)=\sum_{b=1}^{z}\psi_b e^{-i\gamma_{ab}} \quad \text{for all } a. \tag{9}$$

This set of equations in generally referred to as the Alexander equations since they were derived first by Alexander.[13] The number z of nearest neighbors need not be a constant for a given lattice. In the case of the square and hexagonal lattices treated in this paper z is constant if periodic boundary conditions are assumed. However, if the lattice is finite, the nodes at the edges have fewer neighbors than the inside points. Even though the ratio of the number of boundary lattice points to the total number N of lattice points decreases as $1/N$, significant differences remain between the results for infinite and finite lattices even when $N\to\infty$.

Note from Eq. (6) that, if $l/\xi\ll 1$, the modulus of the order parameter varies approximately linearly with s between the two nodes a and b. If the condition $l/\xi\ll 1$ is not fulfilled, Eq. (6) has to be used, which greatly complicates the calculations.

It is clear from Eq. (6) and (8) that it is sufficient to derive and solve equations for the order parameter ψ_a at the lattice points only: ψ on the wires is then completely determined. If the order parameter exhibits a periodicity in the lattice, and a certain number of adjacent plaquettes form the basis of this periodicity, the union of these plaquettes will be called the basic period.

For some simple finite systems and also one infinite system the nonlinear G-L equations have been solved. For the circle, de Gennes[12] derived the solution. His results were confirmed by the experiment of Little and Parks.[14] A "lasso" with an attached straight wire of length in a given proportion to the circle diameter was treated by de Gennes[12] in the linearized approximation. A "Wheatston bridge," i.e., two rectangles with a common side was solved in the full nonlinearized case by Amman, Erdős, and Haley.[11] The infinite ladder (i.e., an infinite linear sequence of identical squares, adjacent squares having a common side) was studied by Larson, Haley, and Erdős.[15] The experiments of Bruyndoncx *et al.*[16] confirm these calculations. Different geometries were investigated experimentally[17] by such as superconducting quantum interference device-type structures[18] and structures composed of s- and d-type superconducting materials.[19,20]

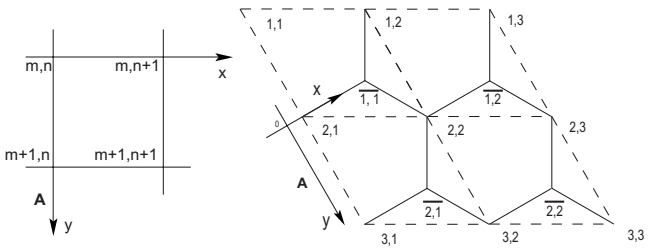

FIG. 1. Coordinate system and node numbering for the square lattice and for the hexagonal lattice. The latter is used to derive the Eqs. (40)–(45). The choice of the vector potential **A** is also shown.

III. EQUATIONS FOR THE ORDER PARAMETER AT THE NODES OF THE SQUARE LATTICE

In this section, we restrict discussion to the square lattice with $z=4$ in Eq. (9) and lattice constant $l=1$. Since the linearized G-L equation, Eq. (2) with $\beta|\psi|^2\psi=0$, is already satisfied by $\psi_a(s)$ as given by Eq. (6), the only conditions left to be satisfied are Eqs. (9). We introduce the abbreviation

$$\epsilon(\xi) = \cos\left(\frac{l}{\xi}\right) \tag{10}$$

and rewrite Eqs. (9) using a notation, that can be understood with reference to Fig. 1.

$$\sum_{\delta} \psi_{m,n+\delta} e^{-i\gamma_{m,n;m,n+\delta}} = 4\epsilon(\xi)\psi_{mn}, \tag{11}$$

where δ is a lattice vector connecting the point (m,n) to one of its neighbors. (In case of ambiguity, lattice point indices are separated by commas and semicolons) The vector potential is chosen as

$$\boldsymbol{A} = (0, Bx, 0). \tag{12}$$

Using Eqs. (7) and (11) we can compute the phase factors $\gamma_{m,n;m,n+\delta}$ and find

$$\gamma_{m,n;m,n\pm1} = 0 \tag{13}$$

and

$$\gamma_{m,n;m\pm1,n} = \mp \frac{2\pi}{\phi_0} Bl^2 n = \mp 2\pi\phi n, \tag{14}$$

where $\phi = Bl^2/\phi_0$ is the magnetic flux though one elementary cell (plaquette) in multiples of ϕ_0. Hence Eq. (11) becomes

$$\psi_{m+1,n}e^{-2\pi in\phi} + \psi_{m-1,n}e^{+2\pi in\phi} + \psi_{m,n+1} + \psi_{m,n-1} = 4\epsilon(\xi)\psi_{mn}. \tag{15}$$

At this point we consider the lattice as obeying periodic boundary conditions in the x and y directions but without specifying the number of its points. One may expect that at a given flux ϕ the set of Eqs. (15) will not have a solution for every value of $\epsilon(\xi)$. If it does have a solution, this means that there exists a nonzero coherence length $\xi(T)$ and a superconducting state of the network. Since the G-L theory is only valid close to T_c, one is dealing with the coherence length $\xi(T_c)$, hence Eq. (4) determines the critical temperature as

$$T_c(B) = T_c(B=0)\left[1 - \frac{\xi^2(T=0)}{\xi^2(T_c)}\right] \tag{16}$$

with

$$\xi_c \equiv \xi(T_c) = l \arccos \epsilon \tag{17}$$

For a given flux ϕ there may exist several values of ϵ for which Eq. (8) possesses a solution. In this case, we suppose that superconductivity will exist up to the highest solution of Eqs. (11) and (16) for T_c, which, in turn, corresponds to the largest value of ϵ. The other solutions of ϵ are then devoid of physical significance since they belong to temperatures much below T_c, where the linearized G-L theory is not valid.

For an infinite lattice it is not clear how to ascertain the existence of solutions. For the lattice with periodic boundary conditions the solutions of Eq. (15) were first studied by Hofstadter[21] in relation with other physical problems. It is nonetheless useful to discuss these solution in detail since we will describe some important properties of them which have not been noticed before and which will be used in this work.

If we assume

$$\psi_{m+N,n} = \psi_{m,n}, \tag{18}$$

$$\psi_{m,n+N} = \psi_{m,n}, \quad N \text{ integer} \tag{19}$$

the "Ansatz"

$$\psi_{m,n}(k_y) = \psi_n(k_y)e^{2\pi ik_y m} \tag{20}$$

inserted into Eq. (15) leads to Harper's equation[22]

$$2\cos 2\pi(n\phi + k_y)\psi_n(k_y) + \psi_{n+1}(k_y) + \psi_{n-1}(k_y) = 4\epsilon(k_y)\psi_n(k_y). \tag{21}$$

The condition Eq. (18) requires

$$e^{2\pi ik_y N} = 1,$$

$$k_y = \frac{k-1}{N}, \quad k = 1, \ldots, N \tag{22}$$

and Eq. (19) implies

$$\psi_{n+N} = \psi_n. \tag{23}$$

Formulating Eq. (21) for ψ_{n+N} and using Eq. (23) shows that a solution of the form Eq. (20) can only exist if $\cos 2\pi[(n+N)\phi + k_y] = \cos 2\pi(n\phi + k_y)$, i.e.,

$$\phi = \frac{k'}{N}, \quad k' = 0, \ldots, N-1. \tag{24}$$

For nonrational values of ϕ, the ansatz, Eq. (20), does not yield a solution. This non rational case will be discussed in another section. Here we assume that Eq. (24) holds. If k' and N have a common divisor, say r, such that $N=rq$, $k'=rp$, the Eqs. (21) for $n=1,\ldots,q$ suffice to determine all ψ_n $(n=1,\ldots,N)$, since the equations for ψ_{n+rq} are identical with these for ψ_{n+q}, for any integer r.

Therefore, in the rest of this paper, we assume

$$\phi = \frac{p}{q}, \quad p,q \text{ relatively prime integers} \tag{25}$$

and the set of Eqs. (21) reduces to q equations, wherein the subscript n is to be taken *mod* q.

This means that the order parameter $\psi_{m,n}$ is assumed to be periodic in the y direction with period q times the lattice constant. We further assume the same period in x direction because this leads to numerous simplifications. From Eq. (18) it then follows that the condition Eq. (22) is replaced by

$$k_y = \frac{k-1}{q}, \quad k = 1, \ldots, q. \tag{26}$$

If we do not assume the same periodicity in the x direction as in the y direction some of the equations will change but the basic features of the solutions remain the same. This conclusion is based on detailed calculations performed on lattices with low values of N and N', where N' is the periodicity in the complementary direction. One change that occurs is the loss of symmetry in the eigenvalues, which do not necessarily occur in pairs of opposite sign.

IV. SOLUTIONS OF THE LINEARIZED G-L EQUATIONS FOR SELECTED VALUES OF THE MAGNETIC FLUX FOR THE SQUARE LATTICE

In accordance with Eqs. (22) and (25), Eq. (20) may be written for a given $\phi = p/q$ as

$$\psi_{n-1}(k) + a_n(k)\psi_n(k) + \psi_{n+1}(k) = \epsilon_{p/q}(k)\psi_n(k), \quad n = 1, \ldots, q \tag{27}$$

with

$$a_n(k) = 2\cos\frac{2\pi}{q}(pn + k - 1), \quad k = 1, \ldots, q \tag{28}$$

and it is understood that $a_n(k)$ and $\psi_n(k)$ depend on p and q as well. We shall call $\epsilon^{(i)}_{p/q}(k)$ the eigenvalues and $\Psi^{(i)}(k) = \{\psi^{(i)}_1(k), \ldots, \psi^{(i)}_q(k)\}$ the eigenvectors. Certain symmetry properties of the set of Harper's Eqs. (27) and (28), are helpful in the determination of its eigenvalues and eigenvectors. These are described in the Appendix.

For certain rational multiples $\phi = p/q$ of the flux quantum we give the eigenvalues $\epsilon^{(1)}_{p/q}$ $(i = 1, \ldots, q)$ and the eigenvectors $\Psi^{(i)} = \{\psi^{(i)}_1, \ldots, \psi^{(i)}_n\}$ for $k = 1$. According to Sec. IV, the other eigenvectors for the same $\epsilon^{(i)}_{p/q}$ and for $k = 2, \ldots, q$ are then constructed by permutation of the components of $\Psi^{(i)}$, Eq. (A4).

A state with periodicity q of the order parameter in the x and y directions, and with a definite critical temperature will then be described by giving the order parameter $\Psi_{mn}[\epsilon^{(1)}_{p/q}]$ in every node as a linear combination of the form

$$\Psi_{mn}[\epsilon^{(1)}_{p/q}] = \sum_{k=1}^{q} c_k \psi^{(1)}_{mn}(k), \quad m,n = 1, \ldots, q \tag{29}$$

and

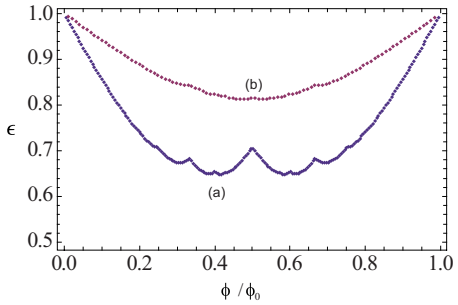

FIG. 2. (Color online) (a) The largest eigenvalues ϵ of Eq. (15) for the square lattice, used in the calculation of the superconducting transition temperature through Eqs. (16) and (17). (b) shows ϵ for the hexagonal lattice, obtained from Eq. (52) or (62). In both cases, ϵ is given as a function of the magnetic flux ϕ per plaquette for rational multiples of the flux quantum.

$$\psi^{(1)}_{mn}(k) = \psi^{(1)}_n(k)e^{2\pi ikm}, \quad k = 1, \ldots, q, \tag{30}$$

where $\epsilon^{(1)}_{p/q}$ is the largest eigenvalue of Harper's Eq. (21) and $\psi^{(1)}_n(k)$ are the components of the eigenvectors belonging to $\epsilon^{(1)}_{p/q}$. The complex coefficients c_k are arbitrary. The largest eigenvalue determines the superconducting transition temperature as a function of the magnetic flux [see Eqs. (16) and (17)] The dependence of this eigenvalue on the flux for the square and for the hexagonal lattices is plotted in Fig. 2. The calculation for the latter lattice is described in Sec. VI.

V. SUPERCURRENT

Slightly below T_c superconductive currents may flow in certain wires of the network. These are calculated from the second G-L equation as

$$J = \frac{e\hbar}{m^*}\Psi^*(s)\left(-i\frac{d}{ds} - \frac{2\pi}{\phi_0}A_s\right)\Psi(s) + \text{c.c.}, \tag{31}$$

where s is the arc-length parameter at any point along the wire. Using Eq. (6) for the order parameter $\psi(s)$ one finds for the current J^x_{mn} directed from the lattice point m,n, toward the lattice point $m,n+1$

$$J^x_{m,n} = \frac{2e\hbar}{m^*}\frac{1}{\xi_c \sin(l/\xi_c)}\text{Im}\{\Psi^*_{mn}\Psi_{m,n+1}\}. \tag{32}$$

The current from the lattice point m,n toward the lattice point $m+1,n$ is

$$J^y_{m,n} = \frac{2e\hbar}{m^*}\frac{1}{\xi_c \sin(l/\xi_c)}\text{Im}\{\Psi^*_{mn}\Psi_{m+1,n}e^{-2\pi i\phi n}\}. \tag{33}$$

Here, x and y indicate the directions of the current according to our convention (cf. Sec. II) and the phase factor in $J^y_{m,n}$ is due to the choice of the gauge, Eq. (12), for the vector potential [cf. also Eq. (14)]. Since we will only compare currents in different wires, we will express the current henceforth in units of $(2e\hbar/m^*)/[\xi_c \sin(l/\xi_c)]$.

If one calculates the currents flowing when the network is in one of its eigenstates with the highest critical temperature, that is, when

$$\psi_{mn} = \psi_n^{(1)}(k) e^{2\pi i k m}, \tag{34}$$

Equations (32) and (33) show that there are no currents in the x direction, whereas along all wires in the y-direction currents flow, whose magnitude depends on the x coordinate, n, through

$$J_{mn}^{y} = \psi_n^{(1)}(k)^2 \sin\frac{2\pi}{q}(k-1-pn). \tag{35}$$

In particular, the sum of these currents over $n=1,\ldots,q$ is zero.

If the network is in a state which is a superposition of the eigenstates belonging to the eigenvalue $\epsilon_{p/q}^{(1)}$, as given by Eqs. (29) and (30), the currents, calculated from Eq. (32) and (33) will be given by a real bilinear form of the complex coefficients c_k, and nothing definite can be said about the corresponding current pattern, since the linearized G-L equations allow any values of the c_k. In the next section it will be shown how the application of the principle of minimal free energy of the superconductor can be used to determine the coefficients c_k and the current patterns.

VI. SOLUTIONS OF THE LINEARIZED G-L EQUATIONS FOR SELECTED VALUES OF THE MAGNETIC FLUX FOR THE HEXAGONAL LATTICE

The regular hexagonal (or honeycomb) lattice is topologically equivalent to a square lattice in which certain branches have been removed as shown. For our purpose it is more convenient to ignore this equivalence and formulate the problem keeping the hexagonal geometry and index the lattice points as shown in Fig. 1.

Making use of the fact that the lattice can be partitioned in two interpenetrating sublattices, we use the same indexing for the two sublattices, called in the sequel red (online, black in print) and blue (online, gray in print), respectively, denoting with a bar over the symbol all quantities which refer to the blue sublattice. The x and y axes and the origin of the coordinate axes are chosen as shown in Fig. 1. This choice simplifies the calculations.

The vector potential A is along the y axis and is taken as $A=(0,Bx,0)$. The length l of each wire connecting adjacent lattice points is taken as $l=1$ so that the flux through each hexagon is

$$\phi = \frac{3\sqrt{3}}{2}B. \tag{36}$$

For periodic boundary conditions the equations of Alexander[13] for the order parameter on the two sublattices are

$$\sum_{\bar{m}',\bar{n}'} \bar{\psi}_{\bar{m}',\bar{n}'} \exp(-i\Gamma_{m,n;\bar{m}',\bar{n}'}) = 3\epsilon\psi_{m,n}, \quad \text{all } m,n \tag{37}$$

and

$$\sum_{m',n'} \psi_{m',n'} \exp(-i\Gamma_{\bar{m},\bar{n};m',n'}) = 3\epsilon\bar{\psi}_{\bar{m},\bar{n}}, \quad \text{all } \bar{m},\bar{n} \tag{38}$$

with

$$\epsilon = \cos\frac{l}{\xi}. \tag{39}$$

The exponents $\Gamma_{m,n;\bar{m}',\bar{n}'}$ and $\Gamma_{\bar{m},\bar{n};m',n'}$, forthwith called phases, are defined as

$$\Gamma_{m,n;\bar{m}',\bar{n}'} = \frac{2\pi}{\phi_0}\int_{(m,n)}^{(\bar{m}',\bar{n}')} \boldsymbol{A}\cdot d\boldsymbol{s} \tag{40}$$

and

$$\Gamma_{\bar{m},\bar{n};m',n'} = \frac{2\pi}{\phi_0}\int_{(\bar{m},\bar{n})}^{(m',n')} \boldsymbol{A}\cdot d\boldsymbol{s}, \tag{41}$$

where the line integral is taken between two adjacent nodes connected by a wire. For clarity, we denote by $\psi_{m,n}$ and $\bar{\psi}_{\bar{m},\bar{n}}$ the order parameters on the red and blue sublattices, respectively. The sum is always carried out over the three nearest neighbors of the given site m,n (or $\bar{m},\bar{n}$).

With the help of the Fig. 1 the phases can be expressed as

$$\Gamma_{m,n;\bar{m}',\bar{n}'} = (\delta_{m,\bar{m}'}\delta_{n-1,\bar{n}'} - \delta_{m-1,\bar{m}'}\delta_{n-1,\bar{n}'})\Gamma(n-1) \tag{42}$$

and

$$\Gamma_{\bar{m},\bar{n};m',n'} = (\delta_{\bar{m}+1,m'}\delta_{\bar{n}+1;,n'} - \delta_{\bar{m},m'},\delta_{\bar{n}+1,n'})\Gamma n \tag{43}$$

with $\Gamma=\pi\phi/\phi_0$. The Alexander Eqs. (4) and (5) reduce to

$$\bar{\psi}_{\bar{m}-1,\bar{n}-1}e^{i\Gamma(n-1)} + \bar{\psi}_{\bar{m},\bar{n}-1}e^{-i\Gamma(n-1)} + \bar{\psi}_{\bar{m}-1,\bar{n}} = 3\epsilon\psi_{m,n} \tag{44}$$

and

$$\psi_{m+1,n+1}e^{-i\Gamma n} + \psi_{m,n+1}e^{i\Gamma n} + \psi_{m+1,n} = 3\epsilon\bar{\psi}_{\bar{m},\bar{n}}. \tag{45}$$

Since lattice points which lie on the borders of the $q\times q$ basic period are connected by one or two wires also to lattice points outside the borders, the subscripts m and n, as well as those with primes and overbar, will always be understood *mod* q in the equations. The number of these equations for the $2q^2$ unknown functions $\psi_{m,n}$, $\bar{\psi}_{\bar{m},\bar{n}}$ can be reduced by a factor of 2 by eliminating $\bar{\psi}_{\bar{m},\bar{n}}$ in Eqs. (44) and (45). This property of bipartite lattices has been already used for the square lattice.

The remaining equations are

$$3\psi_{m,n} + \sum_{m',n'} \psi_{m',n'}B_{m,n;m',n'} = 9\epsilon^2\psi_{m,n}, \quad m,n = 1,\ldots,q \tag{46}$$

with

$$B_{m,n;m',n'} = \exp[i(\Gamma_{m,n;\bar{m}',\bar{n}'} + \Gamma_{\bar{m}',\bar{n}';m',n'})]. \tag{47}$$

The sum in Eq. (46) runs over the six second neighbors on the same sublattice (see Fig. 3). Explicitly

$$\begin{aligned} 9\epsilon^2\psi_{m,n} = {} & 3\psi_{m,n} + \psi_{m-1,n}e^{i2\Gamma(n-1)} + \psi_{m+1,n}e^{-i2\Gamma(n-1)} \\ & + \psi_{m,n-1}e^{i\Gamma(n-1)} + \psi_{m+1,n-1}e^{-i\Gamma(n-1)} + \psi_{m,n+1}e^{-i\Gamma n} \\ & + \psi_{m-1,n+1}e^{i\Gamma n}. \end{aligned} \tag{48}$$

It is clear from Eq. (48) that the roots appear in pairs $\pm\epsilon$ due to the bipartite property of the lattice. As in the square

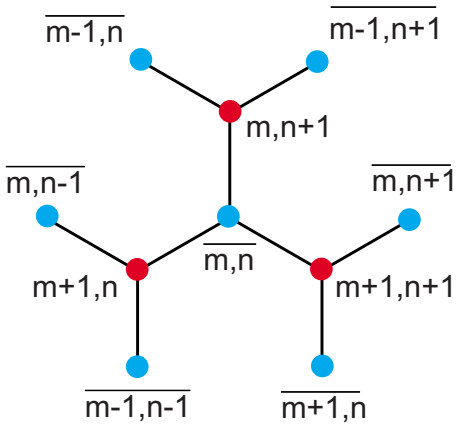

FIG. 3. (Color online) Numbering convention of the points of the hexagonal lattice, showing nearest and next-nearest neighbors of the point $\bar{m},\bar{n}$. Points on the two different sublattices are distinguished by differently colored circles and a bar over the numbers.

lattice we choose a $q\times q$ basic period: in it there are q^2 red and q^2 blue points. The periodicity is expressed by

$$\psi_{m,n}=\psi_{m,n+q},\quad \psi_{m,n}=\psi_{m+q,n} \tag{49}$$

and

$$\bar{\psi}_{\bar{m},\bar{n}}=\bar{\psi}_{\bar{m},\bar{n}+q},\quad \bar{\psi}_{\bar{m},\bar{n}}=\bar{\psi}_{\bar{m}+q,\bar{n}}. \tag{50}$$

The Ansatz

$$\psi_{m,n}=\psi_n e^{ik_y m},\quad k_y=2\pi\frac{k-1}{q},\quad k=1,\ldots,q \tag{51}$$

inserted into Eq. (48) yields

$$9\epsilon^2\psi_n=3\psi_n+2\cos[2\Gamma(n-1)-k_y]\psi_n+2\cos[\Gamma(n-1)-k_y/2]e^{ik_y/2}\psi_{n-1}+2\cos[\Gamma n-k_y/2]e^{-ik_y/2}\psi_{n+1} \tag{52}$$

and the periodicity condition reduces to

$$\psi_n=\psi_{n+q} \tag{53}$$

imposing a constraint on the phase

$$\Gamma q=2\pi p,\quad p=0,1,\ldots. \tag{54}$$

Since $\Gamma=\pi\phi/\phi_0$, this implies, that the Ansatz will yield a solution provided that ϕ is of the form

$$\phi=\frac{2p}{q}\phi_0. \tag{55}$$

The function ψ_n depends on k. There are reciprocal relationships between the function $\psi_{m,n}(k)$ of the red sublattice and the $\bar{\psi}_{\bar{m},\bar{n}}(k)$ of the blue sublattice for the same k, expressed by Eq. (44): once the $\psi_{m,n}(k)$ are determined, $\bar{\psi}_{\bar{m},\bar{n}}(k)$ can be calculated.

As in the case of the square lattice, the greatest eigenvalue ϵ determines the superconducting transition temperature for the given flux ϕ. In the case of the square lattice all eigenvalues were q-fold degenerate and the q eigenvectors, each belonging to a different value of k, were linearly combined with arbitrary coefficients c_k to form a complete set of order parameters $\Psi_{m,n}$. The coefficients c_k were then determined by minimizing the free energy. A peculiarity of the hexagonal lattice is, that while for odd q the eigenvalues are q-fold degenerate, for even q they have only $q/2$-fold degeneracy. In this case, however, always two different k values have common eigenvalues so that the number of equations needed to determine the coefficients c_k is restored to q. To find these coefficients, we impose the condition of minimal free energy (see Sec. VII)

$$\beta=\frac{\sum_{m,n}(|\Psi_{m,n}|^4+|\bar{\Psi}_{\bar{m},\bar{n}}|^4)}{\sum_{m,n}(|\Psi_{m,n}|^2+|\bar{\Psi}_{\bar{m},\bar{n}}|^2)}=\text{Minimum}, \tag{56}$$

where $\Psi_{m,n}=\Sigma_{k=1}^{q}c_k\psi_{m,n}(k)$ and $\bar{\Psi}_{m,n}=\Sigma_{k=1}^{q}c_k\bar{\psi}_{m,n}(k)$. Since $\bar{\Psi}_{\bar{m},\bar{n}}$ are uniquely determined by $\Psi_{m,n}$ through Eqs. (44), the complex coefficients c_k are the same for $\bar{\Psi}_{\bar{m},\bar{n}}$ and $\Psi_{m,n}$.

It turns out that the denominator in Eq. (56) is proportional to $\Sigma_{k=1}^{q}|c_k|^2$. Therefore Eq. (56) is equivalent to minimizing its numerator keeping $\Sigma_{k=1}^{q}|c_k|^2$ constant. Once $c_k(k=1,\ldots,q)$ are known, the currents are calculated from

$$J^{up}_{\bar{m},\bar{n}}=\frac{2e\hbar}{m^*}\frac{1}{\xi_c\sin(l/\xi_c)}\mathrm{Im}[\bar{\Psi}^*_{\bar{m},\bar{n}}\Psi_{m,n+1}e^{i\Gamma n}],$$

$$J^{le}_{\bar{m},\bar{n}}=\frac{2e\hbar}{m^*}\frac{1}{\xi_c\sin(l/\xi_c)}\mathrm{Im}[\bar{\Psi}^*_{\bar{m},\bar{n}}\Psi_{m+1,n}],$$

$$J^{ri}_{\bar{m},\bar{n}}=\frac{2e\hbar}{m^*}\frac{1}{\xi_c\sin(l/\xi_c)}\mathrm{Im}[\bar{\Psi}^*_{\bar{m},\bar{n}}\Psi_{m+1,n+1}e^{-i\Gamma n}]. \tag{57}$$

The superscripts *up*, *le* (left), and *ri* (right) refer to the three wires connected to a given node of the blue (online, gray in print) sublattice, as shown in Fig. 3.

VII. ENERGETICS OF THE SUPERCONDUCTING NETWORK

Since the eigenvalues $\epsilon^{(i)}_{p.q}$ are q-fold (square lattice), respectively, $q/2$-fold (hexagonal lattice) degenerate, any linear combination of the form (29) will give rise to an acceptable spatial distribution of the order parameter Ψ_{mn}. Therefore the question arises what condition will determine the physically realized distribution Ψ_{mn} and the pattern of supercurrents, or, in other words, what determines the coefficients c_k in Eq. (29)? As has been noted, probably for the first time, by Wang,[8] a similar question has already been answered concerning bulk superconductors of the second kind in a magnetic field.[23] In that case the linearized G-L equations yield an infinite degeneracy. Taking into account the nonlinear term in the G-L equations in an approximate but self-consistent manner, Abrikosov minimized the free energy of the bulk superconductor and obtained a state in which the magnetic field penetrates the material at places which form a certain periodic pattern, supercurrents circulat-

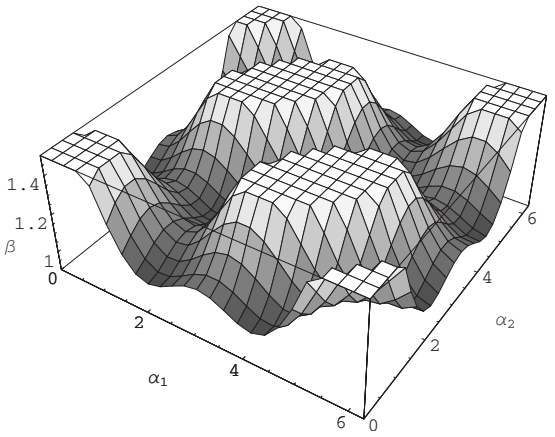

FIG. 4. Three-dimensional view of the free energy F surface parameter β for the square lattice for a magnetic flux $\phi=\phi_0/3$. The free parameters are α_1 and α_2 [Eq. (61)]. The minimum of F fixes the values α_1 and α_2.

inglike vortices around the penetrating field lines. We use the same idea to determine the complex coefficients c_k.

The free-energy density, following Ginzburg and Landau is written as

$$F = F_n + \frac{1}{2m}\left|\left(-i\hbar\nabla - \frac{2e}{c}\boldsymbol{A}\right)\psi\right|^2 + \alpha|\psi|^2 + \frac{1}{2}\beta|\psi|^4 + \frac{1}{8\pi}\boldsymbol{B}^2. \tag{58}$$

As can be seen from the form of the free energy density F, Eq. (58), minimizing F including the fourth order term amounts to the minimization of the parameter β defined in Eq. (56). This leads to the problem of finding the minimum of $\langle|\psi|^4\rangle$ keeping $\langle|\psi|^2\rangle^2$ constant. As shown above, both of these expressions contain the arbitrary constants c_k

$$\langle|\psi|^4\rangle = \frac{1}{2ql}\sum_{m,n}\int|\psi_{m,n}(s)|^4 ds = \frac{1}{ql}\sum_{klmn} t_{klmn} c_k c_l c_m^* c_n^*. \tag{59}$$

The coefficients t_{klmn} are numerical factors determined by the eigenvalue $\epsilon_{p/q}^{(1)}$ and the q eigenvectors found for $\epsilon_{p/q}^{(1)}$, and all sums run from 1 to q. The problem is thus reduced to finding the minimum of the last expression with respect to the variation of the q complex coefficients c_k, keeping $\langle|\psi|^2\rangle$, that is the sum of the squared moduli of the c_k constant. That constant may be chosen without loss of generality equal to 1.

We may consider the set c_k as components of a complex vector in q-dimensional space; the condition

$$\sum_{k=1}^{q}|c_k|^2 = 1 \tag{60}$$

then defines the unit sphere in this space. Hence our task is to minimize the function defined by Eq. (59) over the surface of the unit sphere. Therefore we parameterize the coefficients c_k using q-dimensional complex spherical coordinates and minimize the right hand side of Eq. (59) with respect to these parameters to ensure that Eq. (60) is satisfied.

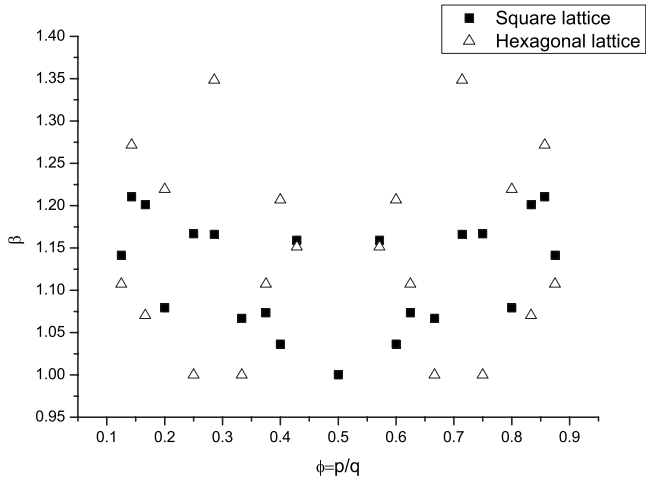

FIG. 5. Plot of the values of β, defined in Eq. (56), that minimize the free energy, as a function of the magnetic flux per plaquette, for rational multiples p/q of the flux quantum. The results for the square lattice are indicated by full squares, for the hexagonal lattice by triangles.

This parameterization takes the following form:

$$c_1 = \cos t_1,$$

$$c_2 = \sin t_1 \cos t_2(\cos\alpha_2 + i\sin\alpha_2)$$

$$\vdots$$

$$c_k = \sin t_1 \sin t_2 \ldots \sin t_{k-1} \cos t_k(\cos\alpha_k + i\sin\alpha_k)$$

$$\vdots$$

$$c_q = \sin t_1 \sin t_2 \ldots \sin t_{q-1}(\cos\alpha_q + i\sin\alpha_q). \tag{61}$$

Hence the number of parameters is $2q-2$. The minimization of $\langle|\psi|^4\rangle$ was carried out using the computer program Mathematica of Wolfram Inc. There are several equivalent minima corresponding to different sets of coefficients c_k. The order parameter patterns ψ_{mn} that correspond to the different sets of c_k can be mapped into each other by the symmetry operations of the lattice hence correspond to the same physical situation.

As an example we show the situation for the square lattice and $q=3$, where it turns out that $t_1=t_2$. Therefore the amplitudes $|\psi_{m,n}^{\min}|$ are equal to each other on all lattice points and only the phase of the order parameter varies with n and m. This means that β may be plotted as a function of α_1 and α_2. Figure 4 shows the equivalent minima of β, and the current pattern that corresponds to one of the minima is shown in Fig. 6.

This minimization process was carried out for the square and hexagonal lattices up to $q=8$ and all p. Because for a given q the cases p/q and $(q-p)/q$ are equivalent (see the Appendix) there are only eight different cases. For the hexagonal lattice, the case $p/q=1/2$ does not exist, because it corresponds to a full flux quantum per plaquette.

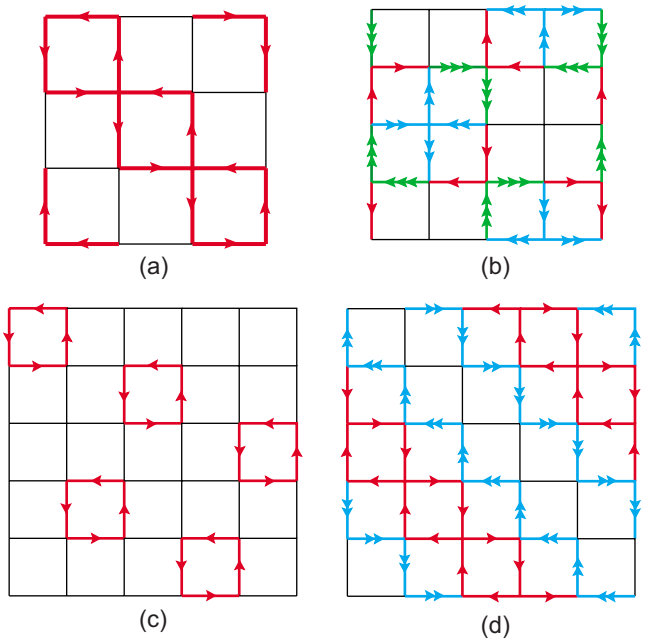

FIG. 6. (Color online) Superconducting current patterns minimizing the free energy for the Square lattice for selected values of the magnetic flux ϕ per plaquette in units of ϕ_0. The patterns are periodic with period q. Currents of different magnitudes are indicated by different numbers of arrows. The direction of the arrows is that of the current flow. The fluxes and the ratios of the currents are given in Table I.

We found that only for $p/q=1/3$, shown above as an example of minimization, are the amplitudes (moduli) of the order parameter equal in all lattice points. In all other cases the amplitudes vary from point to point within the period $q\times q$. This is why a method presuming the constancy of the amplitudes,[24,25] could not give a correct description of the situation, except for $p/q=1/3$.

The results of the minimization for β are shown in Fig. 5. The current patterns for selected fluxes for the square lattice are shown in Fig. 6, these for the hexagonal lattice in Fig. 7.

VIII. STRAIGHTFORWARD SOLUTION METHOD

Another method to solve the equations for the order parameter at the lattice nodes will be illustrated on the example of the hexagonal lattice. In Eq. (48) we consider $\psi_{m,n}$ as a vector of q^2 components arranged in a conveniently fixed order, for instance,

TABLE I. Square lattice current ratios for fluxes $\phi=\frac{p}{q}$. See Fig. 6.

q	p	Current ratios	Figure 6
3	1	$J=0.25$	a
4	1	$J_1/J_2/J_3=0.0345178/0.166667/0.201184$	b
5	1	$J=0.163462$	c
5	2	$J_1/J_2=0.131433/0.172048$	d

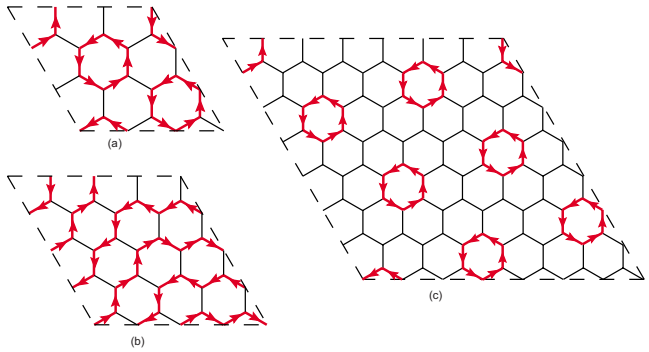

FIG. 7. (Color online) Superconducting current patterns minimizing the free energy for the hexagonal lattice for selected values of the magnetic flux ϕ per plaquette in units of ϕ_0. The patterns are periodic with period q. Currents of different magnitudes are indicated by different numbers of arrows. The direction of the arrows is that of the current flow. The fluxes and the ratios of the currents are given in Table II.

$$(\psi_{11},\psi_{12},\ldots,\psi_{1q},\psi_{21},\psi_{22},\ldots,\psi_{2q},\ldots,\psi_{q1},\psi_{q2},\ldots,\psi_{qq})$$

and rewrite Eq. (48) as a matrix eigensystem equation of order q^2. This contrasts with Harper's equation which gives rise to an eigensystem of order q. Since we solve these equations for larger q numerically, the q^2 equations are just as easy to solve as the q Harper's equations. The advantage gained is that we neither need to introduce the "Ansatz," Eqs. (20) for the square and Eq. (51) for the hexagonal lattice, nor and the parameter k_y (see Secs. III and VI).

In the hexagonal lattice case, the equations Eqs. (48) can be rewritten as

$$9\epsilon^2\psi_{m,n}=3\psi_{m,n}+A_n\psi_{m-1,n}+A_n^*\psi_{m+1,n}+B_n\psi_{m,n-1}+B_n^*\psi_{m,n+1}+C_n\psi_{m-1,n+1}+C_n^*\psi_{m+1,n-1}. \quad (62)$$

Here A_n, B_n, and C_n are defined as follows:

$$A_n=e^{i2\Gamma(n-1)},$$

$$B_n=e^{i\Gamma(n-1)},$$

$$C_n=e^{i\Gamma n}. \quad (63)$$

One obtains a $q^2\times q^2$ matrix equation for the q^2 functions $\psi_{m,n}$ The eigenvalues (ϵ^2-3) and the eigenvectors can straightforwardly be determined, and one finds that the eigenvalues are q-fold degenerate. The order parameter $\Psi_{m,n}$ is constructed by linearly combining the eigenvectors which belong to the largest eigenvalue. For example, for $q=3$

TABLE II. Hexagonal lattice current ratios for fluxes $\phi=\frac{2p}{q}$. See Fig. 7.

q	p	Current ratios	Figure 7
3	1	$J=0.214263$	a
4	1	$J=0.176777$	b
7	3	$J=0.0625374$	c

$$\Psi_{m,n} = c_1\psi^{(1)}_{m,n} + c_2\psi^{(2)}_{m,n} + c_3\psi^{(3)}_{m,n}. \quad (64)$$

Here c_1, c_2, and c_3 are complex coefficients, and $\psi^{(1)}_{m,n}$, $\psi^{(2)}_{m,n}$, and $\psi^{(3)}_{m,n}$ are the three eigenvectors belonging to the largest eigenvalue. Using the set $\Psi_{m,n}$, the free energy can be minimized, and the coefficients c_k are computed as shown in Sec. VII.

IX. DIFFERENT PERIODICITIES OF THE ORDER PARAMETER IN THE *x* AND *y* DIRECTIONS

In Sec. III it was assumed that the order parameter has the period N in the x and y directions. From this we deduced that the phase had to be of the form Eq. (25) with p and q relative primes and $N=rq$ with r and integer for Eq. (20) have a solution. We investigate now what happens if the periodicity in the y direction (i.e., m) is still N but in the x direction (i.e., n) the period is N'. Equations (18) and (22) remain unchanged but Eqs. (19) and (23) change to

$$\psi_{m,n+N'} = \psi_{m,n},$$

$$\psi_{n+N'} = \psi_n \quad N' \text{ integer}.$$

A solution will be obtained only when the flux is a rational multiple of the flux quantum. This implies that Eq. (26) is replaced by

$$k'_y = \frac{k'-1}{N'}, \quad k' = 0,1,\ldots,N', \quad (65)$$

where N' is different from N. Consequently, Harper's equation, Eq. (21), remains valid, with k_y replaced by k'_y. The energy spectrum $\epsilon(k'_y)$ of the modified Harper's equation is different from $\epsilon(k_y)$. We have not exhaustively studied the general case $N \neq N'$; in the cases $N'=N+1$ the following was found: Whereas for $N=N'$ the energy minima are degenerate (see Fig. 4), for $N \neq N'$ they are nondegenerate. It follows, that in the degenerate (symmetric) case a linear combination of the degenerate set of order parameters can be constructed that minimizes the nonlinear term in the free energy (see Sec. VII). In the nondegenerate (asymmetric) case the non linear term in the free energy is fixed and is higher than in the symmetric case.

As examples have calculated the parameter β defined by Eq. (56) for a few simple patterns. The patterns for which β is minimal will be the stable ones. We found for the symmetric 3×3 and 4×4 patterns $\beta(3\times3)=1.0667$ and $\beta(4\times4)=1.1667$, for the asymmetric 2×3 and 3×4 patterns $\beta(2\times3)=1.2887$ and $\beta(3\times4)=1.6875$, respectively. It can be seen that the symmetric patterns have lower free energies than the asymmetric patterns.

X. SEMIINFINITE AND FINITE LATTICES

All results presented hitherto assumed periodic boundary conditions in both the x and y directions. In experiments other boundary conditions will prevail and in this section we discuss how they modify our results. The usual argument to justify periodic boundary conditions is that boundary effects rapidly decay with increasing distance from the boundary in the interior of the sample. However, this argument fails when the current pattern calculated using periodic boundary conditions is such that currents are entering and leaving through the boundaries, except in the case where the sample borders on a conductor that allows the flow of current through the sample. Some of the current patterns obtained using periodic boundary conditions obey automatically the zero boundary current conditions, for instance, for $\phi=\frac{2}{5}\phi_0$ for the square lattice.

If the periodic boundary conditions are retained in one direction, but replaced by finite boundaries in the other direction, we obtain nets of cylindrical shape, like nanotubes. Even though this would require a radial magnetic field that may only be realized by simulation, this case is of interest, because the requirement that the flux be a rational multiple of the flux quantum is not needed to solve the Alexander equations. This can be understood by looking at Eq. (19), which now does not need to be fulfilled. Instead, two of the Harper set of equations are modified containing the edge nodes; the number of neighbors of these nodes is reduced. Since Eq. (19) led to the requirement of fractional fluxes, the Alexander equations can be solved for a continuous set of the variable ϕ.

To handle the case of finite lattices one has to modify the Eq. (15) to take into account the fact that boundary points are connected to a lesser number of nodes than interior points, e.g., in the square lattice corner nodes have two nearest neighbors while other boundary nodes are attached to three neighbors.

Finite size lattices were studied theoretically by Sato and Kato.[26] Their results will be discussed and compared with ours in Sec. XI. Hexagonal and kagome lattice samples that realize the above-mentioned boundary condition with flow through were experimentally studied by Xiao *et al.*[27] through resistivity measurements.

XI. DISCUSSION

As mentioned in Sec. I, there are interesting similarities between the mathematical treatment of superconducting wire lattices on one hand and tightly bound electrons with nearest-neighbor hopping on a lattice on the other hand, both subject to a magnetic field.[28,29] However, there are important differences that should be kept in mind:

First, The Ginzburg-Landau model is nonlinear and this nonlinearity gives rise to the remarkable current patterns. Second, in the tight-binding model the electrons have a dispersion relation $\epsilon(k)$ in even in the absence of a magnetic field due to the lattice potential that modulates the electron density. In contrast, in the Ginzburg-Landau model there is no dispersion relation: the superconducting electron density is uniform in the wires in the absence of a magnetic field.

Third, even if the first Ginzburg-Landau equation is linearized to obtain an approximate solution and the resulting equation has the form of a Schrődinger equation, its solution is not the wave function of an electron subject to Fermi statistics as in the case of the tight-binding model. Hence in our case there are no such parameters as the Fermi level or the

filling factor, which are of great importance in the electronic case.

Despite of these differences both problems lead to a mathematical model described by the Harper equations and therefore our study yields also some iseful results concerning the latter problem, as is shown, e.g., in the Appendix.

In the electron hopping model, when the hopping integrals are the same in all directions, the energy ϵ depends on $B^{1/2}$ for low fields. For the superconducting network we find the same dependence. The tight-binding model on hexagonal lattices in a magnetic field was most recently studied by Dietl *et al.*,[30] where the hopping integrals are different in different directions of hopping. This gives rise to a Hofstadter-type energy spectrum but with a $B^{3/2}$ dependence of ϵ at low fields.

Abrikosov[23] demonstrated that on the surface of a bulk superconductor of the second kind in a magnetic field the hexagonal arrangement of vortices has a lower free energy than a square arrangement. Hence the question arises whether one can similarly assert that the free energy per unit area is smaller in a hexagonal wire lattice than in a square one. Figure 5 gives an indication in this respect: one can see that indeed the lowest free energies are obtained in general but with exceptions, for the hexagonal case.

An approximation method to obtain the maximal eigenvalues, and thereby the critical temperatures, of the linearized G-L equations of a superconducting wire network in a magnetic field has been developed by Lin and Nori.[31,32] For finite lattices the method is even exact. They express the eigenvalues ϵ (see Sec. III) in terms of the sum of the phase factors defined in Eqs. (13) and (14) over all closed paths of length l originating in one lattice point. All sums with all possible values of l are needed and the approximation consists in truncating the calculation at some l. It seems, that the procedure converges adequately; the authors use as many as 10^{96} paths. The advantage of this method is, that it is not restricted to rational values of the flux; instead one obtains the superconducting-normal phase boundary as a continuous function of the magnetic flux. One should be aware of the fact that the continuous curve obtained for ϵ as a function of ϕ has no physical meaning for nonfractional values of the flux, where the denominator q of the fraction is directly related to the length of the path of the path integral. This is analogous to our observation that the eigenvalue spectra for the infinite lattice with periodic boundary conditions as calculated by our direct method not using the Bloch Ansatz have only meaning for fractional values of the flux. This can be seen in the diagrams of these authors demonstrating the self similarity property of the ϵ vs ϕ curves, where the similarity is successively washed out as the size of the similarity intervals is diminished. Since Lin and Nori use the linearized G-L equations and no minimization of the free energy, this method is not suited to calculate the current distribution.

The removal of the periodic boundary conditions and the introduction of sample boundaries has important consequences on the eigenvalue spectrum of the Alexander equations. One general consequence is, that lattices which odd q values and therefore not bipartite become bipartite when finite. Therefore the finite odd cases retain the $\epsilon \rightarrow -\epsilon$ symmetry (see Appendix). This may be seen in the example shown in Fig. 8. Another consequence of the finiteness of the lattice is that the eigenvalue spectrum may be calculated for the whole continuous range of fluxes. It is clear from the Fig. 8 that the highest eigenvalue and with it the character of the highest eigenstate changes at the level crossings. This may give rise to different current and flux patterns, as shown in the upper part of the figure.

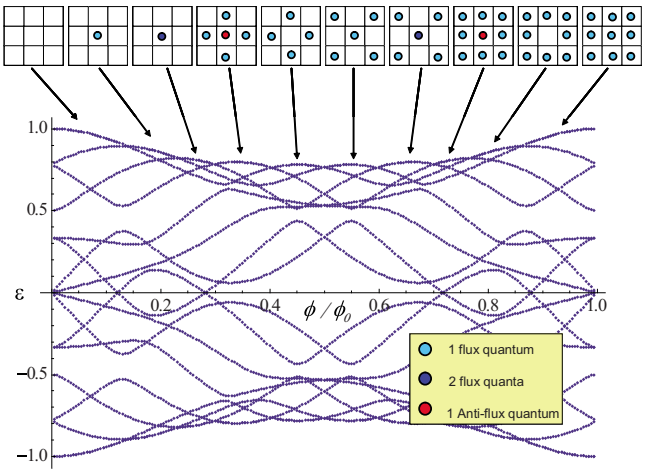

FIG. 8. (Color online) Eigenvalue spectrum of the 3×3 square lattice without periodic boundary conditions hence the flux ϕ does not need to be a rational multiple of ϕ_0. Therefore the spectrum is a continuous function of ϕ. In the top part of the figure the flux patterns are shown for the highest eigenvalue that determines the superconducting transition temperature. The levels cross and therefore the highest eigenvalue changes as a function of flux.

It is interesting to compare the results of Sato and Kato[26] with the ones in this paper. These authors restrict themselves to the linearized Ginzburg-Landau equations and do not attempt to minimize the free energy. They calculate the maximal eigenvalue of the linearized equation and the associated dependence of the superconducting transition temperature on the magnetic field for the infinite square lattice. The result is the same as obtained by the other authors, including us. However, since they do not use any minimization principle to select the appropriate linear combinations of the degenerate eigenvectors belonging to the largest eigenvalue, they resort to finding the distribution of fluxoids from the change of the phase of the order parameter along closed loops. This process does not yield a unique ground state configuration of the order parameter and does nor permit the determination of the distribution of superconducting currents if the largest eigenvalues of the Alexander equations are degenerate. Interesting are the results of these authors concerning finite size lattices, consisting of $n\times n$ lattice points, for $n=10$, 20, and 40. In this situation the highest transition temperature is determined by the order parameter at the boundaries and because of the lack of periodicity the order parameter decreases exponentially toward the center of the cluster. The critical temperature vs field curves so obtained do not approach the curve for the infinite lattice. This is understandable, since the critical temperature is defined here as the temperature at which the superconductivity completely disappears. One may argue that, since the currents in the boundary wires only have to counteract the flux inside the cluster, the edge points

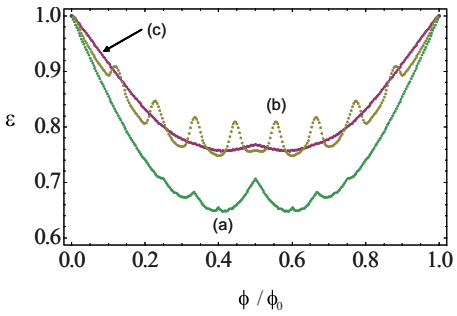

FIG. 9. (Color online) Plots of the eigenvalue spectra for three related square lattices:(a) Infinite square lattice with periodic boundary conditions. (b) Semiperiodic or tubular lattice; it is infinite in one direction and has the period 20 in the perpendicular direction. (c) Finite 20×20 square lattice.

and especially the corner points remain superconducting in higher fields than in the infinite periodic lattice, no matter how large the lattice is.

We observed (see Fig. 9) that even though the ratio of the number of boundary lattice points to the total number N of lattice points decreases as $1/N$, significant differences remain between the results for infinite and finite lattices even when $N\to\infty$. This is likely due the differences in definition used for the superconducting-normal transition point for infinite and finite lattices. Just as in the case of the bulk superconductors of the second kind two transition points are defined characterized by the two critical fields H_{c1} and H_{c2}, for the finite lattice case the critical field is different in the boundary region from that in the interior region (Fig. 10).

ACKNOWLEDGMENTS

One of the authors (P.E.) thanks Stephen B. Haley for introducing him to the problem and for the his early cooperation and discussion of the square lattice case along the lines of the linearized Ginzburg-Landau equations without minimization of the free energy. P. Erdős is especially grateful to School of Science and Engineering of Sun Yat-sen University and Zhibing Li for their warm hospitality during the two authors' collaboration. We also thank Zhibing Li for numerous illuminating discussions and to Hui Zhai for the communication of his results. The support of National Basic Research Program of China (Grant No. 2007CB935500) is gratefully acknowledged.

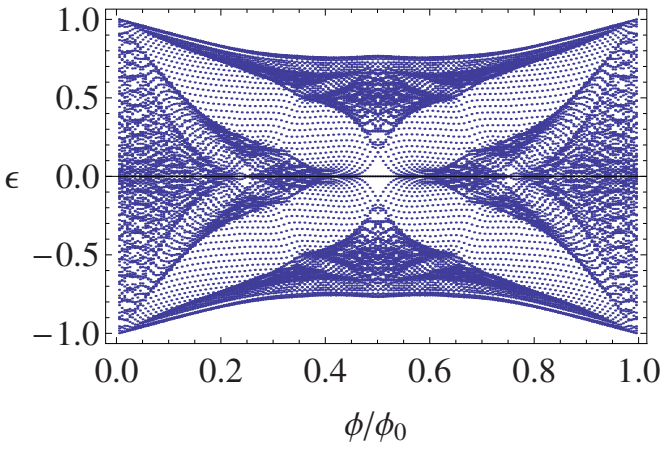

FIG. 10. (Color online) Eigenvalue spectrum for the 10×10 finite square lattice. calculated for 300 equipartioned values of the flux from 0 to ϕ_0. The areas with a scarce distribution of points are in the infinite periodic lattice gaps and are populated by edge states. Due to their presence the highest eigenvalue is moved higher giving rise to a higher transition temperature.

APPENDIX: SYMMETRY PROPERTIES OF THE SET OF HARPER'S EQUATIONS FOR THE SQUARE LATTICE

We refer back to the notation and Equations in the Sec. IV. Without giving the detailed proofs, the following relations hold. For fixed p/q, set $k=1$, $a_n(0)=a_n$, $\epsilon^{(i)}_{p/q}(k)=\epsilon$, and $\psi^{(i)}_n(1)=\psi^{(i)}_n$, because the solutions for $k>1$ will easily follow from those for $k=1$. We note that if q is even (and p is odd since p and q are relatively prime), there exist $q/2$ pairs of integers n, $n'=n+q/2$, with $0<n<n'\leq 1$ such that $\cos\frac{2\pi}{q}pn=-\cos\frac{2\pi}{q}pn'$. Since $a_n=\epsilon+2\cos\frac{2\pi}{q}pn$, inspection of Eqs. (27) and (28) shows that the following replacement leaves the set of equations invariant:

$$\epsilon\to-\epsilon,$$

$$\psi_n\to-\psi_{n'}. \tag{A1}$$

Therefore, for q even the nonzero eigenvalues occur in pairs opposite in sign, which means that the characteristic equation is a function of degree $q/2$ of ϵ^2. Moreover, the components of the eigenvectors which belong to ϵ and $-\epsilon$ are related through Eq. (A1).

Further, we note that

$$a_n=a_{q-n},\quad n=1,\ldots,q-1. \tag{A2}$$

This symmetry leads to the relationship

$$\psi_{q-n}=\psi_n \quad \begin{matrix} n=1,\ldots,\frac{q}{2}-1 & \text{if } q \text{ is even} \\ n=1,\ldots,\frac{q-1}{2} & \text{if } q \text{ is odd} \end{matrix} \tag{A3}$$

for one set of eigenvectors and to a similar relationship, but with minus sign, for the remaining set. As a consequence the secular equation of Eq. (27) is factored into two polynomials of order $\frac{q}{2}+1$ for q even, and of order $\frac{q+1}{2}$ if q is odd for the first set of eigenvalues, and another polynomial of order $\frac{q}{2}-1$ for q even and $\frac{q-1}{2}$ if q is odd. For instance, for $q=7$ the factors are of order 4 and 3. A further simplification occurs when q is a multiple of 4. Since in this case the secular equation factors into two polynomials of odd order in ϵ and it must be an even function of the nonvanishing roots, two of them must be zero.

It turns out that the eigenvalues $\epsilon^{(i)}_{p/q}(k)$ for given p/q and i are q-fold degenerate: they are the same for all $k=1,\ldots,q$. Moreover, the q eigenvectors which belong to an eigenvalue $\epsilon^{(i)}_{p/q}$ (dropping the index k) can be obtained by the following process once one of them has been computed:

$$\psi_n(k+tp) = \psi_{n+t}(k), \quad k = 1, \ldots, q; \quad n = 1, \ldots, q, \quad t \text{ integer}, \tag{A4}$$

where all integers are to be taken mod q. Hence, the eigenvectors for a given eigenvalue and for successive values of k may be obtained by a p-step cyclic permutation of the components of a single eigenvector, most conveniently that for $k=1$.

A further remark simplifies calculations: the matrix of the set of Eqs. (27) and (28) is invariant under the replacement

$$p \rightarrow q - p \tag{A5}$$

therefore the eigenvalues and eigenvectors are the same for p/q and $(q-p)/q$ (e.g., for $\phi=\frac{3}{5}$ and $\phi=\frac{2}{5}$).

*paul.erdos@epfl.ch

[1] T. P. Polak and T. K. Kopeć, Phys. Rev. A **79**, 063629 (2009).
[2] T. Đurić and D. K. K. Lee, Phys. Rev. B **81**, 014520 (2010).
[3] K. Kasamatsu, Phys. Rev. A **79**, 021604(R) (2009).
[4] M. Tinkham, *Introduction to Superconductivity* (McGraw Hill, New York, 1975).
[5] P. G. de Gennes, *Superconductivity of Metals and Alloys* (Addison-Wesley, New York, 1989).
[6] Y. Y. Wang, Ph.D. thesis, Scientific Technological and Medical University of Grenoble, 1987.
[7] B. Pannetier, J. Chaussy, R. Rammal, and J. C. Villegier, Phys. Rev. Lett. **53**, 1845 (1984).
[8] Y. Y. Wang, R. Rammal, and B. Pannetier, J. Low Temp. Phys. **68**, 301 (1987).
[9] P. Gandit, J. Chaussy, B. Pannetier, and R. Rammal, Physica B **152**, 32 (1988).
[10] L. P. Gorkov, Zh. Eksp. Theor. Fiz. **36**, 1918 (1959) [Sov. Phys. JETP **9**, 1364 (1959)].
[11] C. Ammann, P. Erdös, and S. B. Haley, Phys. Rev. B **51**, 11739 (1995).
[12] P. G. de Gennes, C. R. Seances Acad. Sci., Ser. 2 **192**, 279 (1981).
[13] S. Alexander, Phys. Rev. B **27**, 1541 (1983).
[14] W. A. Little and R. D. Parks, Phys. Rev. Lett. **9**, 9 (1962).
[15] T. Larson, S. Haley, and P. Erdös, Physica B **194-196**, 1425 (1994).
[16] V. Bruyndoncx, J. S. Rodrigo, T. Puig, L. Van Look, V. V. Moshchalkov, and R. Jonckheere, Phys. Rev. B **60**, 4285 (1999).
[17] B. Pannetier, J. Chaussy, and R. Rammal, J. Phys. (France) Lett. **44**, 853 (1983).
[18] V. V. Moshchalkov, L. Gielen, M. Dhalle, C. van Haesendonck, and Y. Bruynseraede, Nature (London) **361**, 617 (1993).
[19] M. Fujii, T. Abe, H. Yoshikawa, S. Miki, S. Kawamata, K. Satoh, T. Yotsuya, M. Kato, M. Machida, T. Koyama, T. Terashima, S. Tsukui, M. Adachi, and T. Ishida, Physica C **426-431**, 104 (2005).
[20] T. Ishida, M. Fujii, T. Abe, M. Yamamoto, S. Miki, S. Kawamata, K. Satoh, T. Yotsuya, M. Kato, M. Machida, T. Koyama, T. Terashima, S. Tsukui, and M. Adachi, Physica C **437-438**, 104 (2006).
[21] D. R. Hofstadter, Phys. Rev. B **14**, 2239 (1976).
[22] P. G. Harper, Proc. Phys. Soc., London, Sect. A **68**, 874 (1955).
[23] A. A. Abrikosov, Sov. Phys. JETP **5**, 1174 (1957).
[24] T. C. Halsey, Phys. Rev. B **31**, 5728 (1985).
[25] T. C. Halsey, Phys. Rev. Lett. **55**, 1018 (1985).
[26] O. Sato and M. Kato, Phys. Rev. B **68**, 094509 (2003).
[27] Y. Xiao, D. A. Huse, P. M. Chaikin, M. J. Higgins, S. Bhattacharya, and D. Spencer, Phys. Rev. B **65**, 214503 (2002).
[28] Y. Hasegawa, P. Lederer, T. M. Rice, and P. B. Wiegmann, Phys. Rev. Lett. **63**, 907 (1989).
[29] Y. Hasegawa, Y. Hatsugai, and M. Kohmoto, Phys. Rev. B **41**, 9174 (1990).
[30] P. Dietl, F. Piéchon, and G. Montambaux, Phys. Rev. Lett. **100**, 236405 (2008).
[31] Y. L. Lin and F. Nori, Phys. Rev. B **65**, 214504 (2002).
[32] Y. F. Wang and C. D. Gong, Phys. Rev. B **74**, 193301 (2006).